



## Original Article

# Uncrewed surface vehicle (USV) survey of walleye pollock, *Gadus chalcogrammus*, in response to the cancellation of ship-based surveys

Alex De Robertis , Mike Levine , Nathan Lauffenburger, Taina Honkalehto, James Ianelli, Cole C. Monnahan , Rick Towler, Darin Jones, Sarah Stienessen, and Denise McKelvey

Alaska Fisheries Science Center, National Marine Fisheries Service, National Oceanic and Atmospheric Administration, 7600 Sand Point Way NE Seattle, WA 98115, USA

\*Corresponding author: tel: +1 206 526 4789; e-mail: [Alex.DeRobertis@noaa.gov](mailto:Alex.DeRobertis@noaa.gov)

De Robertis, A., Levine, M., Lauffenburger, N., Honkalehto, T., Ianelli, J., Monnahan, C. C., Towler, R., Jones, D., Stienessen, S., and McKelvey, D. Uncrewed surface vehicle (USV) survey of walleye pollock, *Gadus chalcogrammus*, in response to the cancellation of ship-based surveys. – ICES Journal of Marine Science, 0: 1–12.

Received 30 April 2021; revised 23 July 2021; accepted 27 July 2021.

In 2020, the developing COVID-19 pandemic disrupted fisheries surveys to an unprecedented extent. Many surveys were cancelled, including those for walleye pollock (*Gadus chalcogrammus*) in the eastern Bering Sea (EBS), the largest fishery in the United States. To partially mitigate the loss of survey information, we deployed three uncrewed surface vehicles (USVs) equipped with echosounders to extend the ship-based acoustic-trawl time series of pollock abundance. Trawling was not possible from USVs, so an empirical relationship between pollock backscatter and biomass established from previous surveys was developed to convert USV backscatter observations into pollock abundance. The EBS is well suited for this approach since pollock dominate midwater fishes in the survey area. Acoustic data from the USVs were combined with historical surveys to provide a consistent fishery-independent index in 2020. This application demonstrates the unique capabilities of USVs and how they could be rapidly deployed to collect information on pollock abundance and distribution when a ship-based survey was not feasible. We note the limitations of this approach (e.g. higher uncertainty relative to previous ship-based surveys), but found the USV survey to be useful in informing the stock assessment in a situation where ship-based surveys were not possible.

**Keywords:** acoustic survey, echo survey, *Gadus chalcogrammus*, Uncrewed surface vehicle, USV, walleye pollock

## Introduction

The COVID-19 pandemic resulted in the cancellation of many fisheries surveys worldwide in 2020. This posed a challenge for fisheries management, which relies on timely and consistent abundance estimates of fish stocks to characterize the state of marine ecosystems to support management decisions (ICES, 2020). This was the case for walleye pollock (*Gadus chalcogrammus*) in the eastern Bering Sea (EBS), which support the largest single-species fishery in the United States with recent landings of ~1.3 million tons and a value of ~1.4 billion dollars (Ianelli *et al.*, 2020). The ship-based acoustic-trawl (AT) and bottom trawl surveys used in the stock assessment

(Ianelli *et al.*, 2020) were delayed and subsequently cancelled due to the risk of the virus to the survey crews and the remote communities where crew exchanges and resupply activities occur. In response, we applied recent advancements in uncrewed surface vehicles (USVs) instrumented with calibrated echosounders (e.g. Swart *et al.*, 2016; De Robertis *et al.*, 2019) to conduct a USV-based acoustic survey. The goal was to mitigate the loss of information from pollock midwater abundance surveys used to support management of this important fishery.

In recent years, ocean-going autonomous vehicles and sensors suitable for measuring the abundance of marine organisms have proliferated (Fernandes *et al.*, 2003; Verfuss *et al.*, 2019;

Reiss *et al.*, 2021). USVs using wind and wave power for propulsion are promising for large-scale fisheries surveys (Greene *et al.*, 2014; Swart *et al.*, 2016) due to their long endurance. Initial short-term deployments (Greene *et al.*, 2014) have been extended to >100 days (De Robertis *et al.*, 2019; Chu *et al.*, 2019; Levine *et al.*, 2021), and USVs capable of conducting acoustic surveys are now commercially available (Verfuss *et al.*, 2019). Low-power echosounders suitable for acoustic measurement of fish abundance from USVs have also been developed (Benoit-Bird *et al.*, 2018). These USV systems have matured to the point that, in many cases, the focus of work is transitioning from the development of vehicles and sensors to how these new tools can best be applied to understand the abundance, distribution, and ecology of marine organisms.

The primary limitation of USVs for acoustic surveys of fish abundance is their inability to perform concurrent direct biological sampling to identify acoustic targets (Fernandes *et al.*, 2003). Acoustic methods are currently insufficient to reliably distinguish among fish species and size classes in most operational situations (McClatchie *et al.*, 2000; Bassett *et al.*, 2017; Korneliussen, 2018). As a result, targeted trawl samples are generally used to identify species and size/age composition of acoustic scatterers during ship-based surveys (McClatchie *et al.*, 2000, Simmonds and MacLennan, 2005). However, in some instances, diversity may be sufficiently low that a single species or group dominates acoustic backscatter and species identification may be less of a concern (Geoffroy *et al.*, 2011; Ressler *et al.*, 2015; Reiss *et al.*, 2021). In the case of the EBS, age 1<sup>+</sup> pollock dominate acoustic scattering in deeper parts of the water column to the point that this backscatter can be attributed entirely to pollock (De Robertis *et al.*, 2010; Honkalehto *et al.*, 2011). As a result, acoustic-only measurements in this environment can be translated into a useful index of total pollock abundance (note that this differs from indices of abundance by size/age produced by traditional surveys). For example, an index of total abundance based on backscatter measurements (i.e. no trawl data) collected opportunistically during the bottom trawl survey has been used as an input to the EBS pollock stock assessment since 2011 (Honkalehto *et al.*, 2011). It thus appeared feasible to generate a useful index of pollock abundance from USV acoustic measurements without concurrent trawl sampling.

Here, we describe an effort to apply these recent technological developments to mitigate the loss of information resulting from survey cancellations caused by the COVID-19 pandemic in summer 2020. The goal was to conduct a USV survey to produce an abundance index consistent with that from a conventional ship-based AT survey in time for incorporation into the annual stock assessment. We used three chartered saildrone USVs to estimate the abundance of walleye pollock on the EBS shelf and extend an AT survey time series ordinarily conducted with a research vessel (McCarthy *et al.*, 2020). The primary challenges faced in this effort were (1) the lack of biological information from trawl sampling, (2) the short timeline to provide information for the stock assessment, and (3) generating results comparable to those from conventional ship-based AT surveys with USVs. We describe the rapid and successful adoption of USVs to mitigate the loss of information from a cancelled ship-based AT survey, and highlight considerations relevant for future application of USVs in fisheries surveys.

## Methods

### Approach

The 2020 AT survey of pollock in the EBS was cancelled due to safety concerns associated with the COVID-19 pandemic. Instead,

three chartered saildrone USVs were deployed from Alameda, CA, to the Bering Sea to estimate pollock abundance and distribution. The USVs surveyed the same area ( $3.5 \times 10^5$  km<sup>2</sup>) as recent AT surveys, but transects were spaced farther apart due to time constraints. The USVs measured acoustic backscatter, but population biomass (kg) is used in the stock assessment model. Thus, the USV backscatter measurements were converted to biomass units based on an empirical relationship between pollock backscatter and biomass derived from previous surveys. Finally, the additional uncertainty introduced by the increased transect spacing and the backscatter-to-biomass conversion was investigated via simple simulations.

### USV survey

Three saildrone USVs equipped with echosounders were used to conduct the survey. Saildrones are 7 m long wind-propelled and solar-powered USVs equipped with oceanographic and meteorological instruments (Mordy *et al.*, 2017). The vehicles autonomously follow pre-planned routes and can be monitored and re-tasked via a satellite link.

The USVs followed a curtailed survey plan designed in case an abbreviated ship-based survey had been possible. The survey consisted of 14 transects spaced 74 km apart with a total length of 4727 km (Figure 1). This represents half the sampling density of previous surveys (transects 37 km apart). The transects extended from water depths of ~60–80 m to the shelf break (>1000 m). The average depth was 127 m and 90% of the area was between 65 and 287 m deep. The survey area was divided into three sectors, each covered by a USV proceeding from southeast to northwest. As in previous surveys, the survey was conducted during daytime; the USVs held position between sunset and sunrise. The USVs paused at wind speeds > 12 m s<sup>-1</sup> as wind-mixed air bubbles attenuate the echosounder transmissions at high wind speeds (De Robertis *et al.*, 2019).

Due to travel restrictions, the USVs could not be deployed near the survey area. Instead, they departed on 15–22 May from Alameda, California and sailed 3700 km across the North Pacific to the Bering Sea (Figure 1). The USVs began the survey on 4 July and finished on 20 August, within the date range of previous acoustic surveys in the EBS (Figure S1). After completing the survey, the USVs sailed back to Alameda. The USVs were recovered on 4 October and raw acoustic data were sent by overnight courier for further processing.

The USVs were equipped with a Simrad WBT mini split-beam echosounder equipped with an ES38-18/200-18CR transducer (18° split-beam 38 kHz and 18° single beam 200 kHz) gimbal mounted on the keel at a depth of 1.9 m (De Robertis *et al.*, 2019; Levine *et al.*, 2021). The echosounders continuously transmitted 0.512 ms narrowband signals every 3 sec. Although backscatter data were collected to 1000 m in previous surveys, only a small amount of pollock backscatter was observed >300 m (mean 0.32%, range 0.08–0.67%). We thus chose to record USV data to 300 m to simplify data collection as this required fewer changes to instrument settings during the survey. Raw echosounder data were written to flash memory media, and data summaries were transmitted over the satellite link (De Robertis *et al.*, 2019).

The echosounders were calibrated before and after the survey in San Francisco Bay on 13–14 May and 28 October 2020 following Renfree *et al.* (2019). These calibrations were conducted at warmer temperatures (16.7/18.3°C at the transducer) than encountered during the survey at the transducer depth (mean 10.3°C, 95%

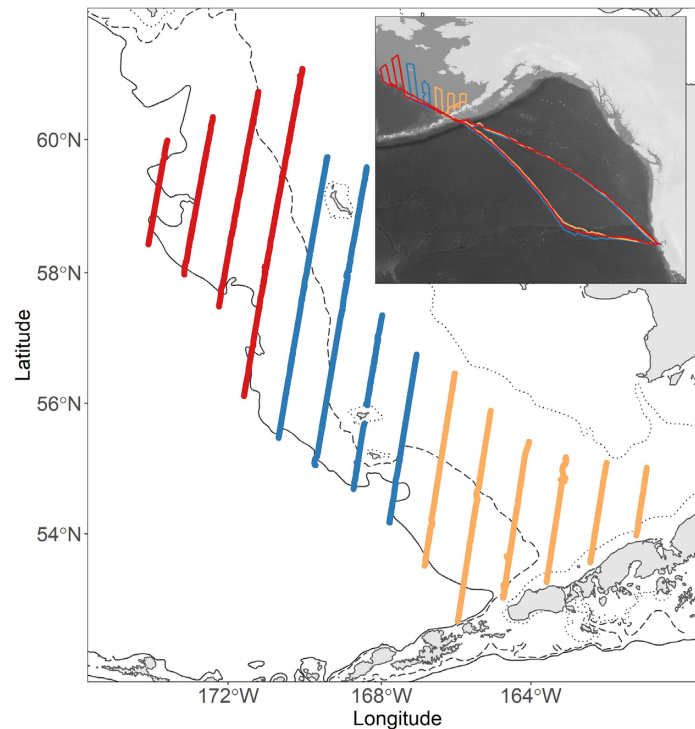


**Figure 1.** USV tracks along the survey transects. Each USV (depicted in a different color) surveyed a series of survey transects spaced 74 km apart starting from the south. The 50, 100, and 200 m depth contours are shown. The inset depicts the path taken by the USVs as they sailed from California across the North Pacific to the survey area and returned.

of observations 8.3–12.8°C), which increases uncertainty due to the potential for temperature-dependent gains (Demer and Renfree, 2008). The mean gain (averaged in the linear domain) from the two calibrations was used in data processing. The pre- and post-survey calibration results were consistent, with gain differing by < 0.1 dB at 38 kHz and < 0.2 dB at 200 kHz for all USVs.

### Processing of acoustic data

The acoustic data were processed using Echoview v11.0 software. Pings exhibiting evidence of attenuation of the transmitted signal by bubbles entrained into surface waters at elevated sea states (i.e. a locally weak bottom echo or variable transmit pulse) were removed following the criteria described in De Robertis *et al.* (2019). The data were processed by four analysts who, as in previous surveys, visually inspected 38-kHz echograms and subjectively attributed backscatter to pollock based on characteristics such as depth distribution (often near-bottom), appearance (consistent with individual fish or schools), frequency response (similar at 38 and 200 kHz), strength of the returned echo (high), and geographic location (scarce in shallow areas). In most cases, acoustic backscatter consistent with fish aggregations in the lower one-third to two-thirds of the water column is dominated by age 1<sup>+</sup> walleye pollock targeted by the survey, and analysts primarily demarcate the depth below which backscatter is attributed to adult pollock (De Robertis *et al.*, 2010; Honkalehto *et al.*, 2011).

In some areas, pollock co-occur with diffuse backscatter from other scatterers making discrimination of pollock and other backscatter more challenging. As in previous surveys (McCarthy *et al.*, 2020), the analysts had the option of applying a two-part filter

to limit the influence of these scatterers prior to assigning backscatter as consistent with pollock. This filter applied a  $-60$  dB re  $1\text{ m}^{-1}$  threshold to limit the influence of weak targets unlikely to be pollock and excluded backscatter with a frequency response outside of 2 standard deviations of that expected for pollock (i.e.  $S_{v,38\text{kHz}} - S_{v,200\text{kHz}} > 7.9$  or  $< -0.9$  dB was excluded; De Robertis *et al.*, 2010). This was applied to 8.5% of the survey and 3.5% of total pollock backscatter was processed in this fashion. Acoustic backscatter attributed to pollock (hereafter pollock backscatter) from consecutive 50-ping intervals was echo-integrated using an integration threshold of  $-70$  dB re  $1\text{ m}^{-1}$  into the nautical area scattering coefficient ( $S_A$ ,  $\text{m}^2\text{ nmi}^{-2}$ ) in the two layers used in previous surveys:  $>3$  m (16 m below the surface to 3 m above the bottom detection), and  $<3$  m (3 to 0.5 m above the bottom detection).

The course of saildrones depends on wind speed and direction as they must tack back and forth to sail upwind, and they drift when becalmed. The distance traveled on a given pre-planned transect thus depends on the wind (e.g. a longer distance will be traveled upwind due to the indirect path), and each along-track interval thus represents a variable distance along the intended transect. We accounted for this potential bias by averaging the processed USV observations into 0.5 nmi (926 m) along-track elementary distance sampling units (EDSUs) defined along the pre-planned intended transects so that each EDSU represented a consistent distance along the intended transect. More 50-ping intervals were associated with each EDSU at low speeds and when traveling upwind. On average, 7.6 intervals were associated with each EDSU (90% of EDSUs in the range of 3–17 intervals). The average number of pings per EDSU for the saildrones ( $\sim 380$ ) is comparable to the number of pings transmitted by a ship transiting at  $6\text{ m s}^{-1}$  (300).

### Adjustment for USV beam width

The USVs were equipped with wider beam transducers (17.0–17.9°) than the 7.0° transducers used in previous surveys. A wider beam leads to a larger near-bottom acoustic dead zone (ADZ) where backscatter from fish cannot be discriminated from the seafloor. The USVs are thus expected to detect less backscatter near the seafloor than the research vessel. The magnitude of this bias depends on the range to the seafloor, the degree to which fish aggregate near the seafloor, and the transducer beam width (Ona and Mitson, 1996). The unobserved backscatter in the ADZ was estimated by computing the mean height of the ADZ and extrapolating the backscatter observed immediately above the ADZ (i.e. the layer extending from 0.5 to 2 m above the bottom echo) into the unobserved volume using the method of Ona and Mitson (1996). The survey time series does not include such a correction for the ADZ. Thus, USV observations were corrected to the ADZ expected for the 7.0° transducer used in previous surveys to maintain consistency with earlier results. This was accomplished by adding the difference between the backscatter estimated in the ADZ for the USV and the research vessel (RV) to the USV observation in the 0.5 to 3 m above bottom layer:

$$s_{A,corr} = s_{A,obs} + (s_{A,ADZ,USV} - s_{A,ADZ,RV}). \quad (1)$$

Survey-wide, this correction increased total pollock backscatter by 3.2%.

### Backscatter to biomass conversion

Pollock biomass is the primary quantity of interest for stock assessment. Trawling was not possible during the USV survey, and measurements of pollock backscatter needed to be converted to biomass units without trawl sampling. We thus examined 16 previous AT surveys of pollock in the EBS conducted between 1994 and 2018 (McCarthy *et al.*, 2020) to determine whether a consistent relationship to convert between pollock backscatter and biomass could be derived.

Pollock dominated the weight of fish caught in pelagic trawls during these surveys (mean = 98.1%, range 95.2–99.8%). Note that large medusae, mostly *Chrysaora melanaster*, which accounted for 7.4% (range 1.0–16.4%) of total catch weight were excluded from the calculations as they are negligible contributors to backscatter relative to fish with swimbladders (De Robertis and Taylor, 2014). Pollock also dominate catches in the summer commercial fishery which is conducted largely in the survey area (Ianelli *et al.*, 2020): pollock accounted for an average of 98.8% of total catch by weight from 2000–2020 (range 97.6–99.4%). In summer 2020, when the USV survey was conducted, the proportion of pollock in the fishery catch was 97.8%. Together, these catch records suggest that acoustic scattering from fish aggregations in this region of the Bering Sea is dominated by pollock.

In the AT surveys, pelagic observations (>3 m) are treated differently than demersal observations (<3 m). Targeted midwater trawl samples are used to convert pelagic backscatter from 16 m below the surface to 3 m above the seafloor to fish abundance (McCarthy *et al.*, 2020). Demersal backscatter, where fishes are more diverse and pollock tend to be larger, is converted to biomass based on species and size composition from a concurrent bottom trawl survey and estimates of species-specific contributions to acoustic backscatter (Lauffenburger *et al.*, 2017). Pollock lengths from trawl catches are used to convert backscatter to fish abundance using a

target strength to length relationship (Traynor, 1996), and biomass is determined by multiplying abundance by weight-length relationships determined from the trawl catches.

For each survey, indices of the total acoustic backscattering cross section attributed to pollock [ $A_T = \sum_i \frac{s_{A,i}}{4\pi} E_i$ , (m<sup>2</sup>), hereafter referred to as total backscatter] and the total pollock biomass [ $B_T = \sum_i B_i E_i$ , (kg)] were computed from observations of  $s_A$  (m<sup>2</sup> nmi<sup>-2</sup>), or biomass density (kg nmi<sup>-2</sup>), at each 0.5 nmi (926 m) EDSU,  $i$ , and the area represented by each EDSU  $E_i$  (20 nmi<sup>2</sup>). As previous surveys exhibited a consistent relationship between total pollock backscatter,  $A_T$ , and biomass,  $B_T$ , linear regressions with an intercept of zero (see results for details) were used to estimate  $C$  (kg m<sup>-2</sup>), a unit conversion used to convert the 2020 USV backscatter observations to pollock biomass (i.e.  $B_T = C \times A_T$ ). As in previous surveys, the midwater (>3 m), and demersal (<3 m) backscatter observations were converted to biomass units using separate relationships.

To examine the potential prediction errors associated with this conversion, we conducted a leave-one-out cross-validation exercise in which the biomass in each survey year was predicted based on the backscatter to biomass relationship observed in the other years. In each year, the survey biomass estimate (i.e. backscatter converted using trawl samples) was compared to that estimated using backscatter to biomass conversions established with observations from the other years as described above.

### Uncertainty estimates

Uncertainty in the EBS pollock survey is quantified using a 1D geostatistical method based on transect biomass sums (Williamson and Traynor, 1996). The resulting “relative estimation error” accounts for uncertainty due to unobserved spatial structure and measurement error on the abundance estimate. If this uncertainty can be assumed to be normally distributed, it provides an estimate of the coefficient of variation (i.e.  $CV = \sigma/K$ ) where  $K$  is the estimated abundance and  $\sigma$  is the square root of the estimation variance associated with the degree of spatial sampling. This assumption is warranted for the EBS AT survey as two times the 1D CV results in an approximate estimate of the 95% confidence interval of precision for this survey (Walline, 2007). We followed this approach to produce an uncertainty estimate comparable to those from previous surveys. Given that fewer transects were sampled in 2020 than in previous surveys, and that backscatter was converted to biomass based on the historical survey results rather than directed trawl samples, one would expect the resulting uncertainties to be larger in the 2020 USV survey.

The 1D method was applied to backscatter in the >3 m and <3 m layers independently. The results were combined assuming independent variances [as the estimated variances in previous years from the 1D method computed for >3 m and <3 m were not significantly correlated ( $r = 0.21$ ,  $p > 0.40$ )]:

$$CV_{total} = CV(A_{T,<3m} + A_{T,>3m}) = \frac{\sqrt{\sigma^2_{<3m} + \sigma^2_{>3m}}}{A_{T,<3m} + A_{T,>3m}}, \quad (2)$$

where  $\sigma^2$  is the estimated variance and  $A_T$  is total pollock backscatter.

We characterized the potential effects of using 74 km rather than 37 km transect spacing in the 2020 survey by comparing backscatter estimates from previous surveys calculated using half the transects (i.e. even or odd numbered transects) with estimates using all



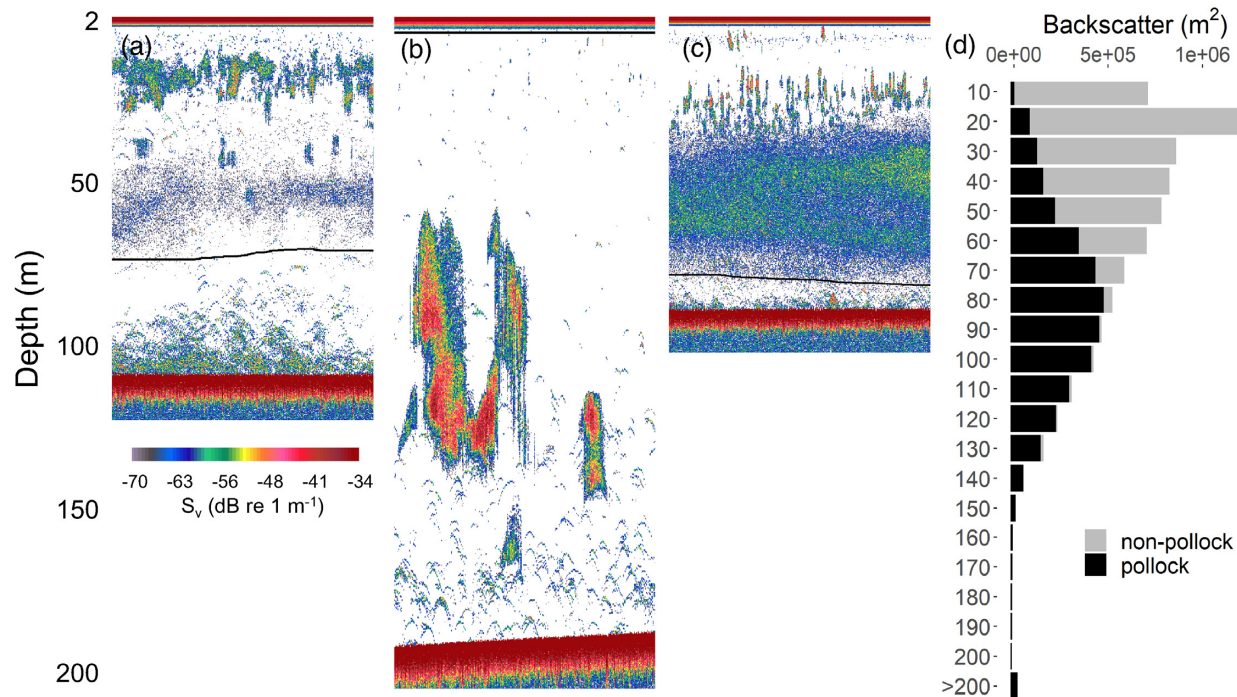


**Figure 2.** Example echograms from the USV survey: (a) pollock in the lower one-third of the water column, (b) a high-density pollock aggregation with few other scatterers, (c) a challenging case where other scatterers dominate the water column and only backscatter close to the seafloor is attributed to pollock. All backscatter was attributed to pollock in panel (b), and backscatter below the black line was attributed to age1<sup>+</sup> pollock in panels (a) and (c). (d) Stacked bars depicting survey-wide daytime depth distribution of pollock backscatter as a function of depth from the surface. The proportion of backscatter attributed to pollock increases with depth.

transects (37 km spacing). The absolute % difference

$$d = \left| \frac{A_{T,\text{all}} - A_{T,\text{half}}}{A_{T,\text{all}}} \right| \times 100, \quad (3)$$

between the total backscatter at all and half transect spacing was used to characterize the discrepancies. For each survey, we computed the 1D CV for backscatter measurements based on all transects (i.e. 37 km transect spacing as in previous surveys), and compared this to the result of using only the odd- or even-numbered transects (i.e. 74 km spacing as in the 2020 survey).

The 2020 USV survey lacked trawl sampling and thus incorporated a backscatter-to-biomass conversion based on the average relationships observed in previous surveys. We accounted for the additional uncertainty introduced by this conversion by propagating the estimated uncertainty in the conversion using a Monte-Carlo simulation. We first drew a random sample  $j$  of total backscatter based on the estimated survey backscatter  $A_T$  and its uncertainty (i.e.  $A_{T_j}'$  is drawn from a normal distribution with mean of  $A_T$  and a SD corresponding to  $A_T$  multiplied by the 1D CV). This step accounts for uncertainty associated with spatial sampling. We then added additional uncertainty to account for the backscatter-to-biomass conversion. Specifically we sampled  $C_j'$  from a normal distribution with a mean corresponding to  $C$  and a SD corresponding to the standard error of the prediction interval from the regression described in the results section. This step accounts for the uncertainty in the biomass that we might have observed in 2020, given the backscatter to biomass relationships from previous years. Biomass is computed as

$$B_{T_j}' = A_{T_j}' \times C_j'. \quad (4)$$

This process was repeated for each of  $10^5$  replicates  $j$ . The CV of the USV survey biomass was estimated from the mean and standard deviation of all replicates  $B_{T_j}'$ . This approach accounts for the reduced sampling in 2020 (as 1D CV will be higher) and the additional uncertainty introduced by the backscatter to biomass conversion.

## Results

### USV survey

The USVs completed the survey without issue. Wind speeds during the survey were modest, averaging  $5.4 \pm 2.5 \text{ m s}^{-1}$  (mean  $\pm$  SD) with 95% of wind speeds  $< 9.7 \text{ m s}^{-1}$ . The USVs travelled at an average speed of  $0.9 \pm 0.5 \text{ m s}^{-1}$ , achieving a maximum speed of  $3.0 \text{ m s}^{-1}$ . Acoustic data were collected throughout the deployment. The geographic distribution of acoustic backscatter was similar to that in previous surveys (Figure S2). The vertical distribution was also consistent with previous surveys (De Robertis *et al.*, 2010; McCarthy *et al.*, 2020). In general, there was a layer of shallow backscatter that was not attributed to pollock, and a near-seafloor layer of backscatter that was attributed to age 1<sup>+</sup> pollock (Figure 2a). In some cases, scattering was attributed almost entirely to age 1<sup>+</sup> pollock (Figure 2b), and in others, scattering from other sources occupied most of the water column (Figure 2c). The strong backscatter from fish schools near the surface (e.g.  $< 40 \text{ m}$  in Figure 2a, c) is typically dominated by age-0 pollock (McKelvey and Williams, 2018). The principal scatterers in the more diffuse backscatter below these schools ( $\sim 40\text{--}75 \text{ m}$  in Figure 2a, c) remain poorly characterized, but these layers often have a different frequency response from pollock (De Robertis *et al.*, 2010). Sampling with pelagic trawls and

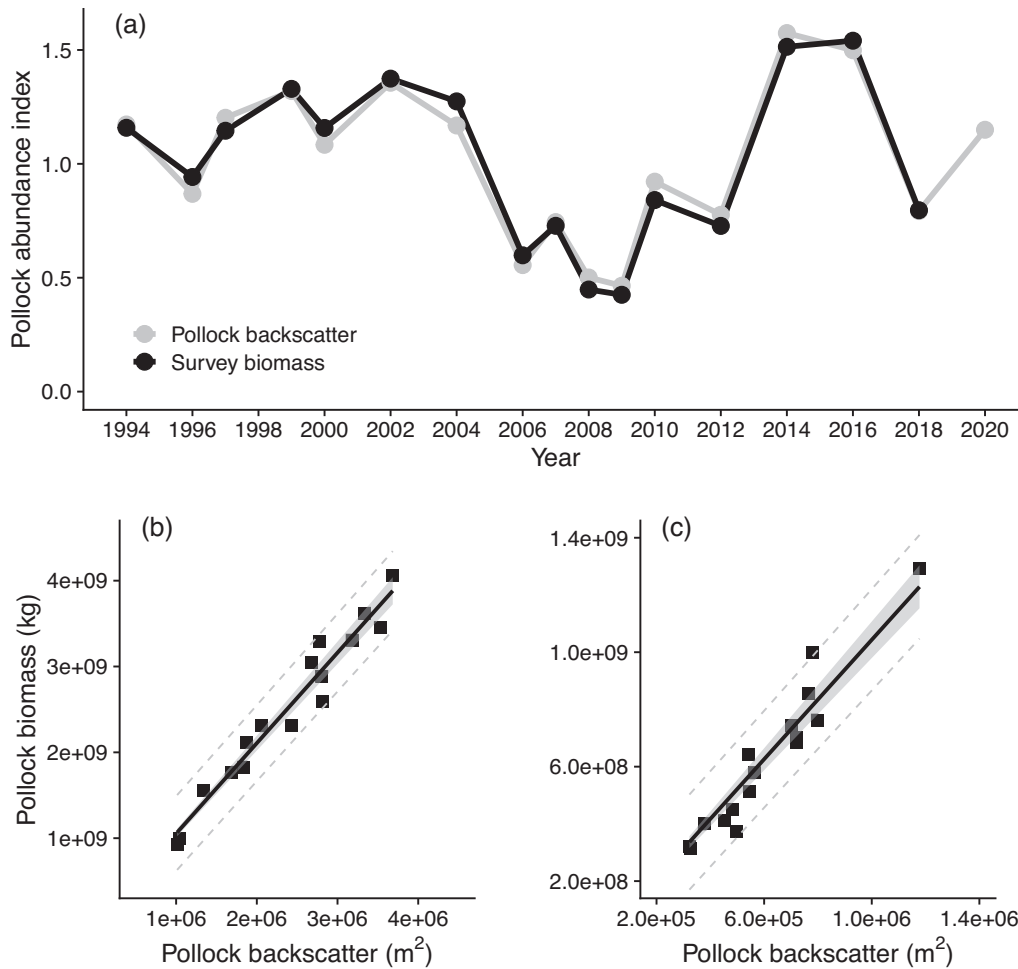


**Figure 3.** Comparison of pollock backscatter and survey biomass in previous EBS AT surveys. (a) Pollock backscatter and biomass for each survey. Observations have been normalized to have a mean of 1 from 1994 to 2018. The 2020 backscatter observation is from the USV survey. The lower panels show the relationship between total pollock backscatter ( $A_T$ ) and biomass ( $B_T$ ) computed based on trawl sampling (b)  $>3$  m above bottom and (c) 0.5 to 3 m above bottom layers. Each point represents a different year. The black line represents a linear regression, with gray shading representing the 95% confidence interval for the expected relationship, and the gray dotted lines represent the 95% prediction interval of the regression (i.e. confidence intervals for a future observation).

trawl-mounted cameras indicates that age-1<sup>+</sup> pollock are scarce in these two scattering layers (McKelvey and Williams, 2018, McCarthy *et al.*, 2020). Survey-wide, 45.0% of the backscatter was attributed to pollock, which is similar to previous surveys ( $48.6 \pm 16.5\%$ , range 23.0–85.3%). As in previous surveys, pollock were more abundant near the seafloor, with few pollock detected near the surface. The majority of backscatter  $>70$  m was attributed to pollock (Figure 2c).

### Backscatter to biomass conversion

Pollock backscatter in previous surveys exhibited a similar trend as pollock biomass (Figure 3a). This suggests that it may be possible to estimate survey-wide pollock biomass reasonably well without trawl information. Linear regression of survey-wide pollock backscatter ( $A_T$ ) and pollock biomass ( $B_T$ ) indicates that backscatter is well correlated with biomass in both the  $>3$  m layer (Figure 3b,  $B_T = 1053.7 \text{ kg/m}^2 \cdot A_T$ ,  $r^2 = 0.99$ ,  $p < 0.001$ ), and the  $<3$  m layer (Figure 3c,  $B_T = 1043.3 \text{ kg/m}^2 \cdot A_T$ ,  $r^2 = 0.99$ ,  $p < 0.001$ ).

Cross-validation revealed that in previous surveys, pollock biomass could be estimated reasonably well with this conversion approach without trawl information in a single year (i.e. Figure 3b and c). Overall, the survey biomass estimated using the conversion exhibited a comparable trend as the conventional survey biomass (Figure 4,  $r^2 = 0.97$ ). The average absolute value of the discrepancy between the survey and the converted estimate was 5.6%, with a range of 0.1 to 12.3%.

Acoustic backscatter from only odd or even transects from previous surveys (74 km spacing) produced similar results as all transects (37 km spacing, Figure 5a), suggesting that the 74 km spacing used in the USV survey was sufficient to capture the primary trends in the abundance time series. The average absolute discrepancy in survey-wide backscatter at 74 km and 37 km spacing was  $3.9 \pm 2.5\%$  (mean  $\pm$  SD). The average 1D CV from 74 km spacing was  $0.097 \pm 0.039$ , which is 2.0 times larger than the average CV ( $0.049 \pm 0.020$ ) in previous years when the survey was conducted at 37 km spacing (Figure 5b). The 1D CVs were high in 1999 and 2008–2009 (Figure 5b) when pollock abundance was low and distributions were restricted to deeper water in the northwest part of

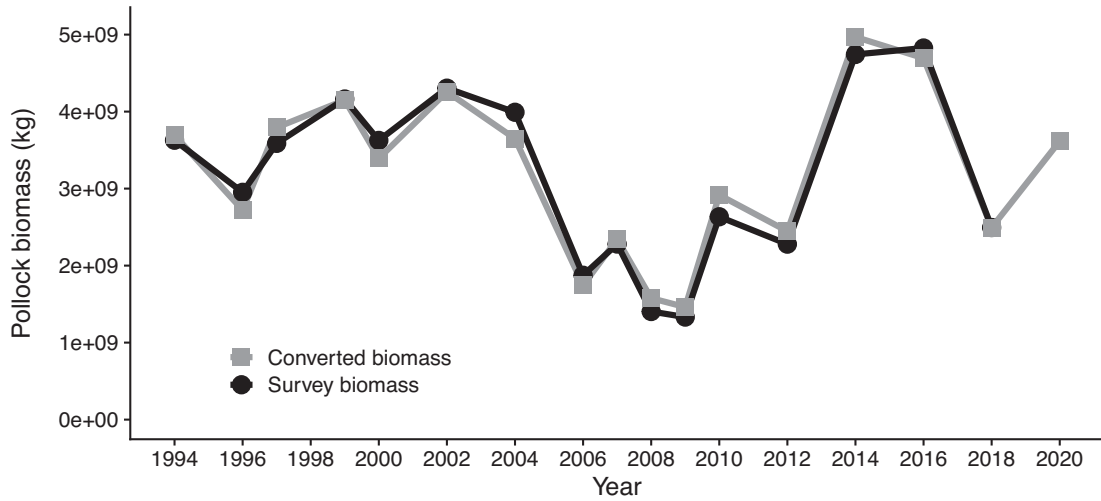


**Figure 4.** Results of cross-validation exercise comparing previous survey estimates (survey biomass) with those in which pollock backscatter in each year is converted to biomass with empirical relationships derived from other years (converted biomass).

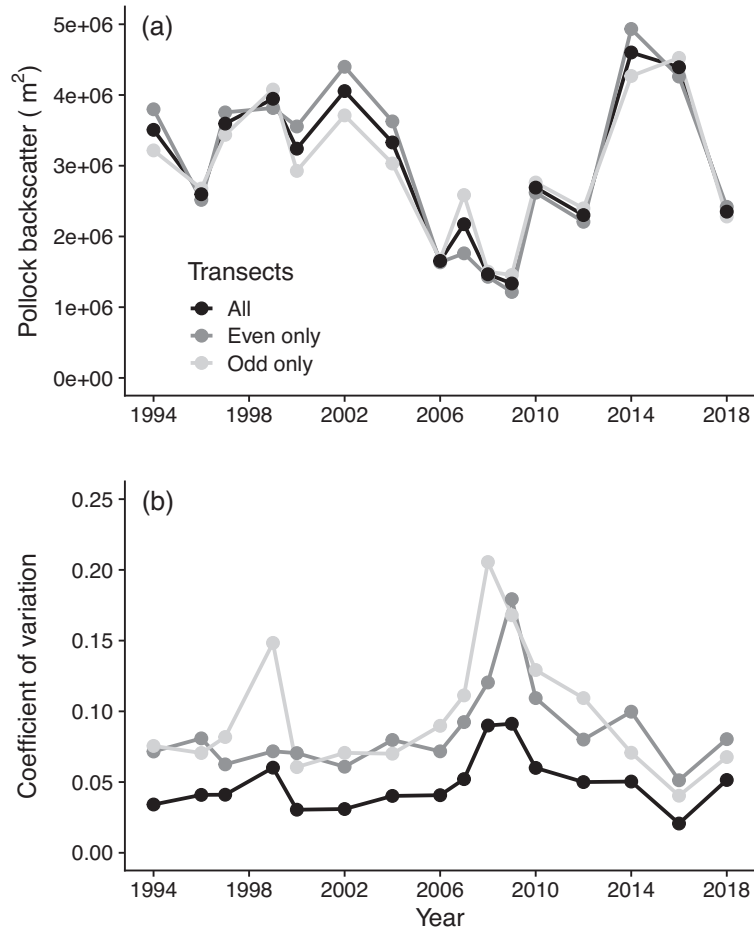


**Figure 5.** Effect of increasing transect spacing on (a) total pollock backscatter ( $A_T$ ) and (b) 1D geostatistical CV estimate in previous pollock AT surveys. Results are shown for the full sampling effort (37 km transect spacing), and the 74 km transect spacing sampled in the 2020 USV survey (i.e. using even or odd numbered transects only).

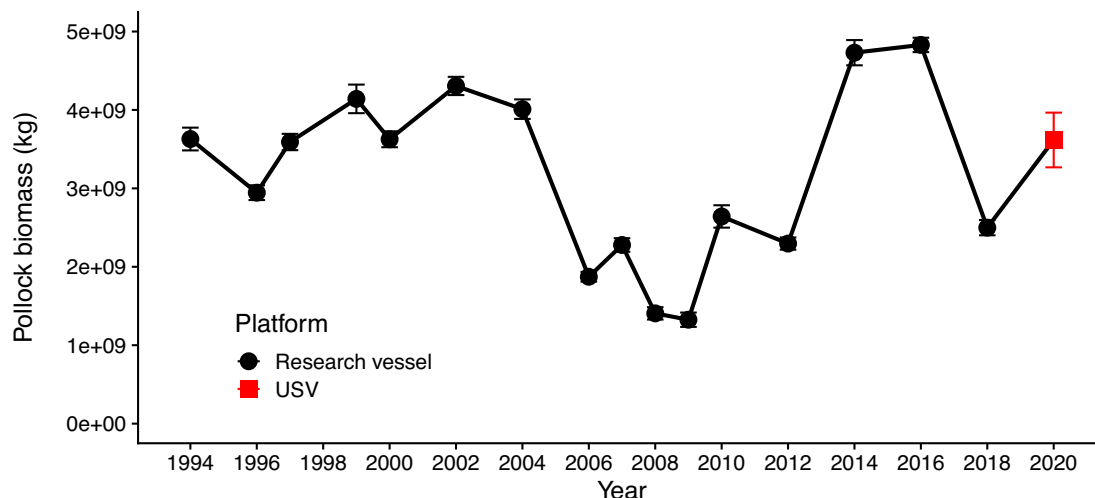


**Figure 6.** Time series of EBS pollock AT abundance estimates. The 2020 estimate (red square) was conducted with USVs at half the transect spacing of previous surveys. Error bars show  $\pm 1$  standard error of the estimate based on the geostatistical 1D estimates. The 2020 uncertainty estimate accounts for the increased uncertainty introduced by the backscatter to biomass conversion.

the continental shelf by extensive cold water (Figure S2, see also Stevenson and Lauth, 2019).

### USV abundance estimates

Total pollock backscatter in the survey area ( $A_T$ ) was  $3.44 \times 10^6$  m<sup>2</sup>, 45.0% higher than in the last survey in 2018 (Figure 3a). The spatial distribution of pollock backscatter was consistent with recent surveys, with pollock most abundant in the northwest portion of the survey area (Figure S2). The biomass estimate for 2020 was  $3.62 \times 10^9$  kg of pollock, which represents an increase of 44.7% relative to the estimate of  $2.49 \times 10^9$  kg in the last survey in 2018 (Figure 6). The CV based on the 1D geostatistical estimate for backscatter measurements in 2020 was 0.068, which is similar to previous surveys reduced to 74 km spacing (Figure 5b). The CV increased to 0.096 when the additional uncertainty of the backscatter to biomass conversion was incorporated (Figure 7). Thus, for the 2020 survey, the uncertainty attributed to spatial sampling is about twice that of the backscatter to biomass conversion. The overall CV is 2.3 times the average CV of 1994–2018 time series (0.042, Figure 6). The proportion of backscatter (15.3%) in the lower 3 m was in the range observed in previous years (11.7–30.2%, Figure S3), which suggests that after correction, the difference in beam width between the USV and the research vessels used for previous surveys did not introduce major bias.

## Discussion

### USV pollock survey

This work used USVs instrumented with echosounders (Swart *et al.*, 2016; De Robertis *et al.*, 2019) to continue a survey time series after the unexpected cancellation of an AT survey. Multiple USVs were used to perform the survey within the time window of previous ship-based surveys to minimize the impact of potential stock migration on survey results. Previous experience working with these USVs (De Robertis *et al.*, 2019; Meinig *et al.*, 2019) allowed for the rapid development and execution of the survey as it became clear that the vessel-based surveys could be cancelled.

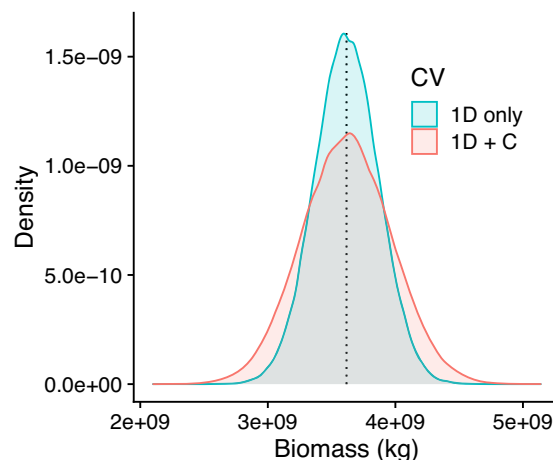


**Figure 7.** Visualization of the Monte Carlo simulation of the 2020 uncertainty estimate. The histograms show the probability density of pollock biomass estimates resulting from the 1D geostatistical error estimate only, and the distribution of biomass estimates when the uncertainty associated with the backscatter to biomass conversion (Figure 3b and c) is added.

Long-term survey time series are a fundamental tool in fisheries management, allowing for fish stock abundance and distribution to be assessed over time (Hilborn and Walters, 2003). Therefore, it is essential that changes to survey methodology be considered in relation to the existing time series, so that direct comparisons to previous surveys remain possible. Where possible, the ship-based AT survey methodology (McCarthy *et al.*, 2020) was followed to produce a comparable USV estimate.

The lack of concurrent biological sampling remains the primary limitation to using acoustic data from USVs to inform fisheries management (Fernandes *et al.*, 2003). In AT surveys, targeted trawl samples are used to allocate backscatter to species and size classes (Simmonds and MacLennan, 2005), which is not feasible from USVs. In some circumstances (e.g. low-diversity high latitude ecosystems) acoustic backscatter can be attributed to species or



important taxonomic groups without additional biological sampling (Geoffroy *et al.*, 2011; Ressler *et al.*, 2015; Reiss *et al.*, 2021). This is the case in the EBS survey area, where pollock account for almost all the backscatter from semi-demersal fishes (De Robertis *et al.*, 2010), and an acoustic-only index is used in the stock assessment (Honkalehto *et al.*, 2011; Ianelli *et al.*, 2020).

The USV survey should not be considered a complete replacement for the AT survey as it does not provide all the information produced by the ship-based survey. For example, estimates of size/age composition and biological measurements from fish specimens, which are important components of this survey (Ianelli *et al.*, 2020) were not possible. The 2020 biomass estimate is also more uncertain than those from previous surveys due to reduced survey coverage and the backscatter to biomass conversion. Most of the increased uncertainty, in this case, is associated with the increased transect spacing rather than the biomass conversion. In addition, the backscatter to biomass conversion approach relies on the assumption that the species and size composition of fishes during the USV survey falls within the range observed in previous surveys. Given these limitations, we plan to conduct future AT surveys of EBS pollock with crewed vessels. However, the USV survey met the intended goal of providing quantitative information on the abundance and distribution of the pollock stock when ship-based surveys were not possible.

### Application to fisheries management

The abundance at age index from the AT survey is critical for providing near-term advice in the stock assessment because historical age compositions indicate that it uniquely provides reliable estimates of “pre-recruit” fish. These younger age groups tend to be more pelagic and more available to the AT survey than bottom trawl surveys (Ianelli *et al.*, 2020). This means that the AT survey provides the first sign of pollock abundance between the ages of 2–4 (full recruitment to the fishery generally is around age 5). Additionally, the AT survey provides a fishery-independent snapshot of pollock distribution throughout the region. This has become increasingly important in tracking the impact of warming and more variable environmental conditions within the Bering Sea (Stevenson and Lauth, 2019; Eisner *et al.*, 2020).

In 2020, the USV survey was the only source of fisheries-independent data available for the EBS pollock stock to the North Pacific Management Council (NPFMC) as the scheduled AT and bottom trawl surveys were cancelled (Ianelli *et al.*, 2020). To extend the existing AT time series with the USV data, it was important to convert the USV-measured acoustic backscatter to total biomass and quantify the additional uncertainty introduced by the use of USVs as described above. Adding the USV data to the assessment model provided assurance that the stock status was stable and suggested a slight increasing trend compared to the previous survey and other model scenarios (Ianelli *et al.*, 2020). The USV data were broadly consistent with other data components fit within the assessment model. Furthermore, the pollock spatial pattern depicted by the USV survey was consistent with the patterns observed in the summer fishery providing additional confidence in the USV results. The assessment model scenario incorporating the USV data was selected by the NPFMC as the basis for management advice.

### Backscatter to biomass conversion

In this study, we derived simple empirical relationships to convert USV backscatter measurements into total pollock biomass. This

conversion was possible because pollock account for most of the observed backscatter from semi-demersal fishes, particularly in the >3 m above the bottom layer where 85% of pollock backscatter was observed in this survey. Given that age-1<sup>+</sup> pollock dominate acoustic scattering from semi-demersal fishes (De Robertis *et al.*, 2010; Honkalehto *et al.*, 2011), much of the variability in the backscatter to biomass conversion is attributable to changes in pollock size distribution. The conversion also exhibits low variability in the <3 m layer where fishes are more diverse, indicating that pollock also account for a high (~80%) and consistent proportion of backscatter across years in this layer (Lauffenburger *et al.*, 2017).

The approach used in this study is equivalent to applying average mass-specific target strengths to convert backscatter to biomass. Backscatter from individual pollock scales as length<sup>2</sup> (Traynor, 1996) and mass scales approximately as length<sup>3</sup> (e.g. McCarthy *et al.*, 2020). Thus, mass-specific scattering is size-dependent and scales approximately as length<sup>-1</sup>. The backscatter-to-biomass conversion for pollock can be thought of as applying an average species and size composition in the absence of trawl samples. When expressed as a mass specific target strength ( $TS = 10 \cdot \log_{10}(C^{-1})$ ) the conversions in this study (−30.2 dB m<sup>2</sup> kg<sup>-1</sup> for both <3 m and >3 m) are very similar to previous estimates derived from target strength measurements and used in early EBS AT surveys (−30 dB re 1 m<sup>2</sup> kg<sup>-1</sup>, Karp and Walters, 1994). The conversion approach used here is potentially applicable to other situations where backscatter can be attributed to species or taxonomic groups without trawl sampling and the average mass-specific target strength is relatively consistent. Existing survey data can be used to estimate the additional uncertainty introduced if a backscatter-to-biomass conversion based on previous surveys is applied (Figure 3).

The consistent relationships between observed backscatter and survey estimates of biomass in EBS pollock surveys indicate that historical changes in species and size/age composition were insufficient to introduce large uncertainties into the backscatter-to-biomass conversion in this survey. However, the use of historical relationships to convert backscatter to biomass assumes that conditions are in the range of those observed historically. In the case of the EBS USV survey, information from the fishery (Ianelli *et al.*, 2020), recent surveys (Eisner *et al.*, 2020), and the spatial and vertical distribution of backscatter observations all indicate that this was the case. However, one should not assume that this assumption will hold over long periods as species distributions change over time (Perry *et al.*, 2005, Stevenson and Lauth, 2019). Thus, the assumptions made in acoustic-only surveys should be periodically confirmed with biological sampling, for example by analysis of fishery data, or alternating USV-based and ship-based surveys.

### Differences between ships and USVs

Fish are known to react to approaching survey vessels, typically biasing survey results lower (De Robertis and Handegard, 2013). Given their small size and lower acoustic and visual stimuli, USVs are likely to elicit fewer behavioral reactions than ships. Although this is an area where USVs are likely to perform better than ships, the potential effects of avoidance behavior must be considered so that changes in avoidance reactions affecting acoustic backscatter are not misinterpreted as changes in stock size. This is of particular concern for surveys of stocks prone to avoidance reactions, and/or distributed close to the surface where avoidance effects tend to be larger (Vabø *et al.*, 2002). It is difficult to predict how fish will behave, but the impact of platform-specific reactions on survey estimates can be quantified by comparing paired measurements under

survey conditions (De Robertis and Handegard, 2013). Comparisons of saildrones and the research vessel used in the EBS survey have shown that both platforms produce equivalent acoustic abundance estimates of pollock (De Robertis *et al.*, 2019).

Hull-mounted echosounders are likely to be mounted shallower on small USVs than on ships. Although shallow transducers increase the detectability of near-surface organisms (Fernandes *et al.*, 2003), they are more subject to signal attenuation from wind-swept bubbles at high sea states (Dalen and Løvik, 1981; Novarini and Bruno, 1982). The saildrone's transducers were mounted at 2 m, while the research vessel used in this survey is equipped with transducers on a drop keel (Knudsen, 2009) extended to 9 m. The potential for weather effects on the USV data was managed by identifying and removing pings with evidence of attenuation as well as pausing the survey at elevated wind speeds (De Robertis *et al.*, 2019). Overall, attenuation of the acoustic signal is unlikely to be a major concern in this case as the survey was conducted in modest wind speeds and sea states. However, this could be a more serious limitation for USV surveys with shallower transducers (Swart *et al.*, 2016) or conducted at higher sea states. Surveys in higher sea states may require deep-towed transducers (Greene *et al.*, 2014), or sub-surface vehicles (Fernandes *et al.*, 2003; Benoit-Bird *et al.*, 2018).

USVs generally support small payloads and it is often necessary to instrument them with compact transducers. Small USVs cannot support the large 38 kHz narrow-beam transducers commonly used for fisheries surveys. Smaller transducers have wider beam widths, and will detect fewer fish near the seafloor. We applied a first-order correction for this effect (Mitson and Ona, 1996) which suggests that a relatively small proportion (3.2%) of the pollock detected by the research vessel were unavailable to the USV. The method assumes a flat seafloor over the beam width, normal incidence, and that fish abundance in the area above the ADZ is equivalent to that within it. In practice, these assumptions are likely to be violated to some degree, resulting in an under-estimate of fish abundance after correction. The survey results are likely robust to modest violations of these assumptions as much of the backscatter is well above the seafloor, and the EBS shelf is relatively shallow and flat (Zimmerman and Prescott, 2018). In cases where organisms are distributed close to the seafloor, at deeper depths, or present in steep or rugose habitat, the ADZ will be larger (Mitson and Ona, 1996) and the use of wider beam transducers may be a more serious limitation.

### Future applications

This work demonstrates that USV deployments can be used to support fisheries management. Instrumented USVs suitable for acoustic surveys are commercially available (Verfuss *et al.*, 2019). In this application, the saildrone vehicles and instrumentation used in this work were leased and the USV company conducted all USV operations and the echosounder calibrations. Given that USVs are increasingly accessible, their use is likely to become more widespread in acoustic survey applications. Before committing to this approach we encourage further analyses. One should quantify the financial cost of and tradeoffs associated with USV-based surveys in comparison to existing or alternate survey strategies. In addition, one should ensure that the resulting data products can fulfill management needs, for example via management strategy evaluation (Punt *et al.*, 2016).

The lack of concurrent sampling of the species and size composition of acoustic scatterers remains the primary limitation to the use of autonomous vehicles in acoustic surveys. In the case of EBS

pollock, we were able to covert backscatter to biomass estimates based on historical relationships, but this will not be possible in many instances. Given the current state of knowledge, USVs equipped with echosounders are likely to be most informative in well-characterized, low-diversity environments. Trawl estimates of species and size composition are critical for most acoustic surveys conducted for fisheries management (Simmonds and MacLennan, 2005). Alternative methods used to infer species and size compositions are, in their current state, insufficient to replace trawl sampling in most fisheries surveys. If USVs are to be used more broadly for fisheries surveys, improved methods to better characterize the species and size composition of acoustic scatterers must be developed.

Trawling is not likely to be possible from autonomous vehicles (Fernandes *et al.*, 2003). Thus, the development of reliable methods to convert acoustic measurements to species and size without trawling has the potential to transform the use of echosounder-equipped USVs. More widespread use of frequency response (Korneliusson, 2018), target-strength measurements (Levine *et al.*, 2021), broadband measurements (Bassett *et al.*, 2017), resonance scattering (Stanton *et al.*, 2012), and application of machine learning (Brautaset *et al.*, 2020; Proud *et al.*, 2020), may ultimately result in better characterization of acoustic targets. Sampling methods that can be adapted to USVs such as small cameras (Fernandes *et al.*, 2016), and environmental DNA samplers (Yamahara *et al.*, 2019; Berger *et al.*, 2020) may prove valuable. It may be useful to incorporate information from predator diets (Reiss *et al.*, 2021) or fishery-dependent biological sampling (McClatchie *et al.*, 2000; Chu *et al.*, 2019), particularly if corrected for size and species selectivity (Millar and Fryer, 1999). Hybrid approaches in which ships and USVs work in tandem, with the ships trawling and the USVs increasing the density of acoustic measurements may prove effective. Survey situations differ, and improvements are likely to be incremental and situation-dependent. A pragmatic approach to select among the many possible approaches is to use simulation (Holmin, 2020) or re-analysis of existing data (Korneliusson, 2016; Proud *et al.*, 2020) to quantify potential effectiveness.

This work, which we believe is the first USV-based survey to be used directly to manage a commercially important fish stock, should be viewed as an early attempt to use USVs to inform fisheries management. The backscatter-to-biomass unit conversion used here is a simple solution to a complex problem that may prove effective in other ecosystems where backscatter from a single species is dominant and historical surveys are available. Although the EBS pollock USV survey could not produce information on species, size, and age compositions typically collected from research vessels, it allowed the AT survey time series to be extended in a situation when gathering such data by other means was not possible.

### Data availability

The data underlying this article are available from NOAA's sonar water column [data archive](https://data.archive.noaa.gov/) at the following DOI's: <https://doi.org/10.25921/a4m9-fa81>, <https://doi.org/10.25921/ntmw-f777>, <https://doi.org/10.25921/875q-9b32>.

### Supplementary Data

**Supplementary figures** S1-S3 are available at the ICESJMS online version of the manuscript.

## Acknowledgments

This work was possible due to Saildrone's extraordinarily capable and rapid implementation of the survey under challenging circumstances. The vision, support, and contributions of many people at NOAA including David Detlor, Michael Gallagher, Robert Foy, Sarah Waugh, Chris Meinig, Tim Gallaudet, Patrick Ressler, Sandra Parker-Stetter, Maggie Mooney-Seus, Jeff Napp, and Cisco Werner made the work possible. This work was supported by NOAA Fisheries' Office of Science and Technology and the Alaska Fisheries Science Center. Reference to trade names does not imply endorsement by the National Marine Fisheries Service, NOAA.

## References

- Bassett, C., De Robertis, A., and Wilson, C. 2018. Broadband echosounder measurements of the frequency response of fishes and euphausiids in the Gulf of Alaska. *ICES Journal of Marine Science*, 75: 1131–1142.
- Benoit-Bird, K. J., Welch, T. P., Waluk, C. M., Barth, J. A., Wangen, I., McGill, P., Okuda, C. *et al.* 2018. Equipping an underwater glider with a new echosounder to explore ocean ecosystems. *Limnology and Oceanography: Methods*, 16: 734–749.
- Berger, C. S., Bougas, B., Turgeon, S., Ferchiou, S., Ménard, N., and Bernatchez, L. 2020. Groundtruthing of pelagic forage fish detected by hydroacoustics in a whale feeding area using environmental DNA. *Environmental DNA*, 2: 477–492.
- Brautaset, O., Waldeland, A. U., Johnsen, E., Malde, K., Eikvil, L., Salberg, A., Handegard, N. O. *et al.* 2020. Acoustic classification in multifrequency echosounder data using deep convolutional neural networks. *ICES Journal of Marine Science*, 77: 1391–1400.
- Chu, D., Parker-Stetter, S., Hufnagle, L. C. Jr., Thomas, R., Getsiv-Clemons, J., Gauthier, S., and Stanley, C. 2019. 2018 Unmanned Surface Vehicle (Saildrone) acoustic survey off the west coasts of the United States and Canada. *OCEANS 2019 MTS/IEEE SEATTLE*. pp. 1–7, doi: 10.23919/OCEANS40490.2019.8962778.
- Dalen, J., and Løvik, A. 1981. The influence of wind-induced bubbles on echo integration surveys. *The Journal of the Acoustical Society of America*, 69: 1653–1659.
- Demer, D. A., and Renfree, J. S. 2008. Variations in echosounder-transducer performance with water temperature. *ICES Journal of Marine Science*, 65: 1021–1035.
- De Robertis, A., and Handegard, N. O. 2013. Fish avoidance of research vessels and the efficacy of noise-reduced vessels: a review. *ICES Journal of Marine Science*, 70: 34–45.
- De Robertis, A., Lawrence-Slavas, N., Jenkins, R., Wangen, I., Mordy, C. W., Meinig, C., Levine, M. *et al.* 2019. Long-term measurements of fish backscatter from Saildrone unmanned surface vehicles and comparison with observations from a noise-reduced research vessel. *ICES Journal of Marine Science*, 76: 2459–2470.
- De Robertis, A., McKelvey, D. R., and Ressler, P. H. 2010. Development and application of an empirical multifrequency method for backscatter classification. *Canadian Journal of Fisheries and Aquatic Sciences*, 67: 1459–1474.
- De Robertis, A., and Taylor, K. 2014. In situ target strength measurements of the scyphomedusa *Chrysaora melanaster*. *Fisheries Research*, 153: 18–23.
- Eisner, L. B., Zuenko, Y. I., Basyuk, E. O., Britt, L. L., Duffy-Anderson, J. T., Kotwicki, S., Ladd, C. *et al.* 2020. Environmental impacts on walleye pollock (*Gadus chalcogrammus*) distribution across the Bering Sea shelf. *Deep Sea Research Part II: Topical Studies in Oceanography*, 181–182: 104881.
- Fernandes, P. G., Copland, P., Garcia, R., Nicosevici, T., and Scoulling, B. 2016. Additional evidence for fisheries acoustics: small cameras and angling gear provide tilt angle distributions and other relevant data for mackerel surveys. *ICES Journal of Marine Science*, 73: 2009–2019.
- Fernandes, P. G., Stevenson, P., Brierley, A. S., Armstrong, F., and Simmonds, E. J. 2003. Autonomous underwater vehicles: future platforms for fisheries acoustics. *ICES Journal of Marine Science*, 60: 684–691.
- Geoffroy, M., Robert, D., Darnis, G., and Fortier, L. 2011. The aggregation of polar cod (*Boreogadus saida*) in the deep Atlantic layer of ice-covered Amundsen Gulf (Beaufort Sea) in winter. *Polar Biology*, 34: 1959–1971.
- Greene, C. H., Meyer-Gutbrod, E. L., McGarry, L. P., Hufnagle, L. C., Chu, D., McClatchie, S., Packer, A. *et al.* 2014. A wave glider approach to fisheries acoustics transforming how we monitor the nation's commercial fisheries in the 21st Century. *Oceanography*, 27: 168–174.
- Hilborn, R., and Walters, C. J. (eds) 2003. *Quantitative Fisheries Stock Assessment: Choice, Dynamics and Uncertainty*. Springer Science and Business Media: Boston, MA. 570p.
- Holmin, A. J., Mousing, E. A., Hjøllø, S. S., Skogen, M. D., Huse, G., and Handegard, N. O. 2020. Evaluating acoustic-trawl survey strategies using an end-to-end ecosystem model. *ICES Journal of Marine Science* 77: 2590–2599.
- Honkalehto, T., Ressler, P. H., Towler, R., and Wilson, C. D. 2011. Using acoustic data from fishing vessels to estimate walleye pollock abundance in the eastern Bering Sea. *Canadian Journal of Fisheries and Aquatic Sciences* 68: 1231–1242.
- Ianelli, J., Fissel, B., Holsman, K., De Robertis, A., Honkalehto, T., Kotwicki, S., Monnahan, C. *et al.* 2020. Assessment of the walleye pollock stock in the eastern Bering Sea. *North Pacific Stock Assessment and Fishery Evaluation Report*. 173 pp. Available at [https://archive.fisheries.noaa.gov/afsc/refm/stocks/plan\\_team/2020/EBSPollock.pdf](https://archive.fisheries.noaa.gov/afsc/refm/stocks/plan_team/2020/EBSPollock.pdf). (Last accessed 8/3/21).
- ICES 2020. *ICES Workshop on unavoidable survey effort reduction (WKUSER)*. *ICES Scientific Reports*. 2:72. . 92pp. <http://doi.org/10.17895/ices.pub.7453>. (Last accessed 8/3/21).
- Karp, W. A., and Walters, G. E. 1994. Survey assessment of semi-pelagic gadoids: the example of walleye pollock, *Theragra chalcogramma* in the eastern Bering Sea. *Marine Fisheries Review*, 56: 8–22.
- Knudsen, H. P. 2009. Long-term evaluation of scientific-echosounder performance. *ICES Journal of Marine Science*, 66: 1335–1340.
- Korneliussen, R., Heggelund, Y., Macaulay, G. J., Patel, D., Johnsen, E., and Eliassen, I. 2016. Acoustic identification of marine species using a feature library. *Methods in Oceanography*, 17: 187–205.
- Korneliussen, R. J. (Ed.). 2018. *Acoustic target classification*. *ICES Cooperative Research Report No. 344*. 104 pp. Available at <http://doi.org/10.17895/ices.pub.4567>. (Last accessed 8/3/21).
- Lauffenburger, N., De Robertis, A., and Kotwicki, S. 2017. Combining bottom trawls and acoustics in a diverse semipelagic environment: what is the contribution of walleye pollock (*Gadus chalcogrammus*) to near-bottom acoustic backscatter? *Canadian Journal of Fisheries and Aquatic Sciences*, 74: 256–264.
- Levine, R., De Robertis, A., Grunbaum, D., Woodgate, R. A., Mordy, C., Mueter, F., Cokelet, E. D. *et al.* 2021. Autonomous vehicle surveys indicate that flow reversals retain juvenile fishes in a highly advective high latitude ecosystem. *Limnology and Oceanography*, 66:1139–1154, doi: 10.1002/lno.11671.
- McCarthy, A., Honkalehto, T., Lauffenburger, N., and De Robertis, A. 2020. Results of the acoustic-trawl survey of walleye pollock (*Gadus chalcogrammus*) on the U.S. Bering Sea Shelf in June - August 2018 (DY1807). *AFSC Processed Report, 2020-07*, 83p. Alaska Fish. Sci. Cent., NOAA, Natl. Mar. Fish. Serv., 7600 Sand Point Way NE, Seattle WA 98115. 92 pp. Available at: <https://repository.library.noaa.gov/view/noaa/27293>. (Last accessed 8/3/21).
- McClatchie, S., Thorne, R. E., Grimes, P., and Hanchet, S. 2000. Ground truth and target identification for fisheries acoustics. *Fisheries Research*, 47: 173–191.
- McKelvey, D., and Williams, K. 2018. Abundance and distribution of ge-0 walleye pollock in the eastern Bering Sea shelf during the Bering Arctic Subarctic Integrated Survey (BASIS) in 2014. U.S. Department of Commerce, NOAA Technical Memorandum NMFS-AFSC-382, 48 p. Available at <http://www.afsc.noaa.gov/Publications/AFSC-TM/NOAA-TM-AFSC-382.pdf>. (Last accessed 8/3/21).



- Meinig, C., Burger, E. F., Cohen, N., Cokelet, E. D., Cronin, M. F., Cross, J. N., de Halleux, S. *et al.* 2019. Public-private partnerships to advance regional ocean-observing capabilities: a saildrone and NOAA-PMEL case study and future considerations to expand to global scale observing. *Frontiers in Marine Science*, 6: Article 448 p 1–15. doi: 10.3389/fmars.2019.00448
- Millar, R. B., and Fryer, R. J. 1999. Estimating the size-selection curves of towed gears, traps, nets and hooks. *Reviews in Fish Biology and Fisheries*, 9: 89–116.
- Mordy, C., Cokelet, E., De Robertis, A., Jenkins, R., Kuhn, C. E., Lawrence-Slavas, N., Berchok, C. *et al.* 2017. Saildrone surveys of oceanography, fish and marine mammals in the Bering Sea. *Oceanography*, 30: 113–116.
- Novarini, J. C., and Bruno, D. R. 1982. Effects of the sub-surface bubble layer on sound propagation. *The Journal of the Acoustical Society of America*, 72: 510–514.
- Ona, E., and Mitson, R. B. 1996. Acoustic sampling and signal processing near the seabed: the deadzone revisited. *ICES Journal of Marine Science*, 53: 677–690.
- Perry, A. L., Low, P., Ellis, J. R., and Reynolds, J. D. 2005. Climate change and distribution shifts in marine fishes. *Science*, 308: 1912–1915.
- Proud, R., Mangeni-Sande, R., Kayanda, R. J., Cox, M. J., Nyamweya, C., Ongore, C., Natugonza, V. *et al.* 2020. Automated classification of schools of the silver cyprinid *Rastrineobola argentea* in Lake Victoria acoustic survey data using random forests. *ICES Journal of Marine Science*, 77: 1379–1390.
- Punt, A. E., Butterworth, D. S., de Moor, C. L., De Oliveira, J. A. A., and Haddon, M. 2016. Management strategy evaluation: best practices. *Fish and Fisheries*, 17: 303–334.
- Reiss, C. S., Cossio, A. M., Walsh, J., Cutter, G. R., and Watters, G. M. 2021. Glider-Based estimates of meso-zooplankton biomass density: a fisheries case study on antarctic krill (*Euphausia superba*) around the northern antarctic peninsula. *Frontiers in Marine Science*, 8: Article 604043 p 1–16. doi.org/10.3389/fmars.2021.604043.
- Renfree, J. S., Sessions, T. S., Murfin, D., Palance, D. K., and Demer, D. A. 2019. Calibrations of wide-bandwidth transceivers (WBT Mini) with dual frequency transducers (ES38-18/200-18C) for saildrone surveys of the California Current ecosystem during summer 2018. U.S. Department of Commerce, NOAA Technical Memorandum NMFS-SWFSC-608. Available at <https://repository.library.noaa.gov/view/noaa/19599>. (Last accessed 8/3/21).
- Ressler, P. H., Dalpadado, P., Macaulay, G. J., Handegard, N., and Skern-Mauritzen, M. 2015. Acoustic surveys of euphausiids and models of baleen whale distribution in the Barents Sea. *Marine Ecology Progress Series*, 527: 13–29.
- Simmonds, E. J., and MacLennan, D. N. 2005. *Fisheries Acoustics*, 2nd Ed. Blackwell Science LTD, Oxford. 437p.
- Stanton, T. K., Sellers, C. J., and Jech, J. M. 2012. Resonance classification of mixed assemblages of fish with swimbladders using a modified commercial broadband acoustic echosounder at 1–6 kHz. *Canadian Journal of Fisheries and Aquatic Sciences*, 69: 854–868.
- Stevenson, D. E., and Lauth, R. 2019. Bottom trawl surveys in the northern Bering Sea indicate recent shifts in the distribution of marine species. *Polar Biology*, 42: 407–421.
- Swart, S., Zietsman, J. J., Coetzee, J. C., Goslett, D. G., Hoek, A., Needham, D., and Monteiro, P. M. S. 2016. Ocean robotics in support of fisheries research and management. *African Journal of Marine Science*, 38: 525–538.
- Traynor, J. J. 1996. Target strength measurements of walleye pollock (*Theragra chalcogramma*) and Pacific whiting (*Merluccius productus*). *ICES Journal of Marine Science*, 53: 253–258.
- Vabø, R., Olsen, K., and Huse, I. 2002. The effect of vessel avoidance of wintering Norwegian spring spawning herring. *Fisheries Research*, 58: 59–77.
- Verfuss, U. K., Aniceto, A. S., Harris, D. V., Gillespie, D., Fielding, S., Jiménez, G., Johnston, P. *et al.* 2019. A review of unmanned vehicles for the detection and monitoring of marine fauna. *Marine Pollution Bulletin*, 140: 17–29.
- Walline, P. D. 2007. Geostatistical simulations of eastern Bering Sea walleye pollock spatial distributions, to estimate sampling precision. *ICES Journal of Marine Science*, 64: 559–569.
- Williamson, N. J., and Traynor, J. J. 1996. Application of a one-dimensional geostatistical procedure to fisheries acoustic surveys of Alaskan pollock. *ICES Journal of Marine Science*, 53: 423–428.
- Yamahara, K. M., Preston, C. M., Birch, J., Walz, K., Marin, R., Jensen, S., Pargett, D. *et al.* 2019. In situ autonomous acquisition and preservation of marine environmental DNA using an autonomous underwater vehicle. *Frontiers in Marine Science*, 6: Article 373 p 1–14. doi.org/10.3389/fmars.2019.00373.
- Zimmermann, M., and Prescott, M. 2018. Bathymetry and canyons of the eastern Bering Sea slope. *Geosciences*, 8: 184.

Handling Editor: Olav Rune Godø